MALAYSIAN JOURNAL OF SCIENCE
MJS
ISSN 1394-3065

Regular Issue

Malaysian Journal of Science 43 (3): 86-97 (September 2024) https://mjs.um.edu.my

INVESTIGATION OF WETTABILITY, ANTIBACTERIAL ACTIVITY, THERMAL INSULATION, AND MECHANICAL CHARACTERISTICS OF ELASTOMER BLEND ADHESIVES WITH HIGH-DENSITY FIBERBOARD WOOD AND ALUMINUM

Maha K. Majeed[1a], Seenaa I. Hussein[2a]*

Abstract: Attention has recently been given to finding alternative and sustainable raw material sources for wood and metal adhesives, such as polyvinyl alcohol (PVA), corn starch (CS), arabic gum (AG), and dextrins (D). Modifying polymer dispersion using unique substances, such as modifying reactive elastomer liquid (EL) using PVA, CS, AG, or D results in sufficiently moisture-resistant adhesive joins. In the present study, the physical characteristics of EL/blended with the natural polymers PVA, CS, AG, and D, based on high-density fiberboard (HDF) wood and aluminum (Al) adhesives and coatings, were investigated and compared to those of pure EL. The EL was blended with PVA, CS, AG, or D at a ratio of 60/40 (w/w) to form EL/blends. The chemical structures, surface and interface morphology, adhesion strengths (including shear strength and pull-off strength), surface roughness, wettings, color intensity, and thermal insulation of the prepared EL and EL/blends were investigated. A scanning electron microscopy (SEM) investigation confirmed filler dispersion and adhesion between the blends, and coated HDF wood, or Al. The developed EL/AG blend had a pull-off strength of 144±5 and 102±3 MPa and a shear strength of 771±11, and 52±3 N with HDF wood and Al substrate, respectively. The EL/PVA blend had a maximum surface roughness value 4.57 µm, and its average water contact angle (WCA) was 85.6°. A plasma jet was used to treat the surface roughness and hence the wettability of the pure EL and the EL/blends, for example, plasma treatment decreased the roughness of the EL/AG blend from 4.36 to 3.28 µm. WCA, and hence wettability, was also significantly influenced by plasma treatment, for example, plasma treatment decreased the WCA of the pure EL from 71.7±0.4° to 30.7±0.7°. The lightness value of the EL/blends was less than that of the pure EL, indicating that (the color adhesives have darkened). Similarly, the yellowness-blueness and redness-greenness values of the EL/blends were greater than those of the pure EL,(rendering the blended adhesives more reddish and bluish). The EL/AG blend was found to have a minimum thermal conductivity (of 0.27 W/m.K), indicating maximum insulation.

Keywords: *Elastomers, adhesives, wettability, mechanical, color, thermal insulation, antibacterial, plasma.*

1. Introduction

Sealant and adhesive substances pervade our environment and are used in almost every company and sector, as a result, significant efforts have been made to develop these compounds (Sunday, 2015; Ali *et al.*, 2021; Almashhadani, 2021; Kun & Pukánszky, 2017). Polar compounds with ionic groups, *i.e.,* hydrophilic molecules, readily absorb and dissolve in polar solvents such as water, where they generate hydrogen bonds. Thus, hydrophilic substances are polar (molecules) that easily establish hydrogen bonds and dissolve in water (Al-Lhaibi & Al-Shabander, 2022).

Natural polymers such as polyvinyl alcohol (PVA), corn starch(CS), and arabic gum (AG), have unique qualities that include non-toxicity, water solubility, and biodegradability, as well as physical traits such as high optical clarity (Hussein *et al.*, 2020; Abd-Elnaiem *et al.*, 2022). Surface coating and engineering boost polymer performance by applying synthesized film coatings, rendering itsuitable for use in energy harvesting, water treatment, and insulating barriers. The relevance of thin layers of polymeric substances on metal production is influenced by various factors such as lightweight and shock-resistant (Ali *et al.*, 2023). Homogeneous or heterogeneous blends of at least two polymers or co-polymers are known as polymer blends or as polymer mixtures. The polymers can interact chemically or physically, and their physical characteristics diverge from those of their parent components (Ali *et al.*, 2021). Polymer blends can be classified into five broad categories, each of which has received extensive research: Thermoplastic-thermoplastic, thermoplastic-rubber, thermoplastic-thermosetting, rubber-thermosetting, and polymer-filler blends (Parameswaranpillai *et al.*, 2014). Elastomers (EL) are polymers that, at typical ambient temperatures, are above their glass transition temperatures and are amorphous in their unstretched condition (Christenson *et al.*, 2005). The EL polymer was utilized in this investigation and had the following characteristics: strong, waterproof, flexible, chemically resistant, and temperature resistant up to 120 °C. They often have low glass transition temperatures, which fall between −50 and −70 °C. A network of cross-links holds the irregularly shaped chain molecules that make up EL together, preventing the chains as a whole from moving around but allowing individual

Authors information:
[a]Physics Department, College of Science, University of Baghdad, Baghdad, IRAQ. E-mail: mahakhalid6431124@gmail.com[1]; seenaa.hussein@sc.uobaghdad.edu.iq[2]
*Corresponding Author: seenaa.hussein@sc.uobaghdad.edu.iq

Received: July 21, 2023
Accepted: September 23, 2023
Published: September 30, 2024

DOI:https//doi.org/10.22452/mjs.vol43no3.10
Malaysian Journal of Science 43(3): 86-97 (September 2024)

chain segments to move locally. The network of cross-links may result from physical connections between chain molecules or covalent bonding (Ebewele, 2000). The method used to synthesize polymer blends affected the structural and mechanical properties of polymer blends especially the adhesion strength (Awaja *et al.*, 2009).

Wood and Al have been used as natural building materials, furniture, tools, vehicles, and ornamental items since the dawn of time due to their distinctive properties and relative availability. Engineers, architects, and carpenters should have more accurate knowledge of wood variation to use it more effectively (Mohammed *et al.*, 2022). High-density fiberboard (HDF) wood is prepared when natural wood has a high density and a low amount of chemical additives. HDF wood is a scientific word that informally means the wood is of high quality and hence expensive (Henke *et al.*, 2022).

Certain polymers are more susceptible to bacterial attack due to the physical qualities of their surfaces or the chemical makeup of the polymer. The microbial population increases in polymers as it is usually used in humid conditions with large levels of organic materials (Hussein *et al.*, 2019). The use of hydrogen peroxide (H_2O_2), a silane coupling agent, and an olefin monomer as an oxidant, a cross-linking agent, and a comonomer, respectively, allowed for the creation of high-performance starch-based wood adhesives (Zhang *et al.*, 2015). It was demonstrated that starch-based wood adhesives' bonding strengths equal 7.88 MPa and 4.09 MPa in dry and wet conditions, respectively. The addition of silicon dioxide (SiO_2) as a filler affected the adhesive qualities of PVA (Hameed, 2016). Their findings revealed that the increases in SiO_2 content, increase the tensile strength and enable it to be used as an adhesive. High-performance, environmentally friendly starch-based glue was synthesized using cassava starch as the primary raw ingredient (Chen *et al.*, 2022). The plywood with modified starch adhesive demonstrated the maximum wet shear strength, 1 MPa, at a pH of 4.5 to 5.5, which was 163% greater than the nontreated starch adhesive.

The need for sustainable and alternative raw materials has increased as a result of the world's energy problems and reliance on petroleum resources. Unfortunately, the limitations include workability at low temperatures, poor water resistance, and limited heat resistance. It is generally known that D, AG, and CS are not moisture-resistant polymers, therefore can be used in damp settings significantly reducing their strength. Adhesive connections that withstand moisture may be created by blending EL and AG, D, PVA, or CS. Therefore, this study aims to improve the shear strength, pull-off adhesions, color intensity, thermal insulation, wearability, and antibacterial activity of EL mixed with naturally mentioned polymers so it may be used for HDF wood and Al coatings and adhesives. In addition, the effect of surface treatment by plasma jet on the wettability and roughness was investigated and compared.

2. Methods and Materials

Materials

The adhesives are EL, and EL blends with AG, D, PVA, or CS. The EL polymer (ρ ~ 1.1 g cm^{-3}) was purchased from Sika Gulf manufactures products in Bahrain. AG is a complex blend of macromolecules with a variety of sizes and compositions, with a high concentration of carbohydrates and a negligibly low concentration of proteins less than 3%. In comparison to other gums, AG has a comparatively low viscosity and a high-water solubility. The D, dextrin, is a white or yellow powder, has ρ equals 1.8 g cm^{-3}, and a boiling point of 865.2 °C. Both the AG and D were purchased from the Chinese company Shanghai Clinical Research Center. PVA is a synthetic polymer that easily dissolves in water, its idealized chemical structure is $[CH_2CH(OH)]_n$, and its ρ equals 1.19 g cm^{-3}. Both PVA and CS have no color (white) and were acquired from the Spanish company Panreac Corn Co., Ltd. The commercially HDF wood and Al adherent substrate were obtained from local markets and their thicknesses are 3 cm and 3 mm, respectively.

Preparation of EL and EL Blends

El and EL/(AG, D, PVA, or CS) blends were produced with weight ratios of 60/40 (w/w). Around 1 g of AG, D, PVA, or CS was suspended, at 70 °C, in 10 ml of deionized water for 1 h while continuously magnetically stirred until the solution became transparent. Then, 40% of the formed solutions were mixed separately with 60% of EL polymer and the mixture was agitated again at room temperature (RT~25°C) for ½ h. The produced samples were then placed into a mold with a 20 cm diameter and fixed at RT for 24 h to ensure full drying and water removal. The thickness of the synthesized polymer layers was calculated by an electronic digital micrometer to be 2 mm.

Characterization

Fourier transform infrared spectroscopy (FTIR) model Shimazu's FTIR-8400S on KBr pellets was used to record an infrared spectrum of EL and EL blends. The FTIR spectrum of EL and EL blends was performed at RT in the range of 4000-400 cm^{-1} to examine chemical bonding between their components. The morphology of the synthesized EL and EL blends, as well as their adherence to HDF wood or Al substrates, were investigated using an SEM model INSPECT S 50 operating at 5 kV.

The PosiTest pull-off adhesion tester was used to evaluate the force required to separate the coating from its substrate as the hydraulic pressure increased. Pressure shown on a digital liquid-crystal display (LCD) shows how effectively the coating clings to the substrate. The PosiTest determines the maximum tensile pull-off force that the coating can bear before detaching (pull-off strength) to evaluate the coating's adhesion. The dolly, adhesive, coating layers, and substrates are among the fractured surfaces that develop along the system's weakest plane and function as breaking points. **Fig. 1** displays the EL and EL blends prepared for the pull-off adhesion test.

DOI:https//doi.org/10.22452/mjs.vol43no3.10
Malaysian Journal of Science 43(3): 86-97 (September 2024)

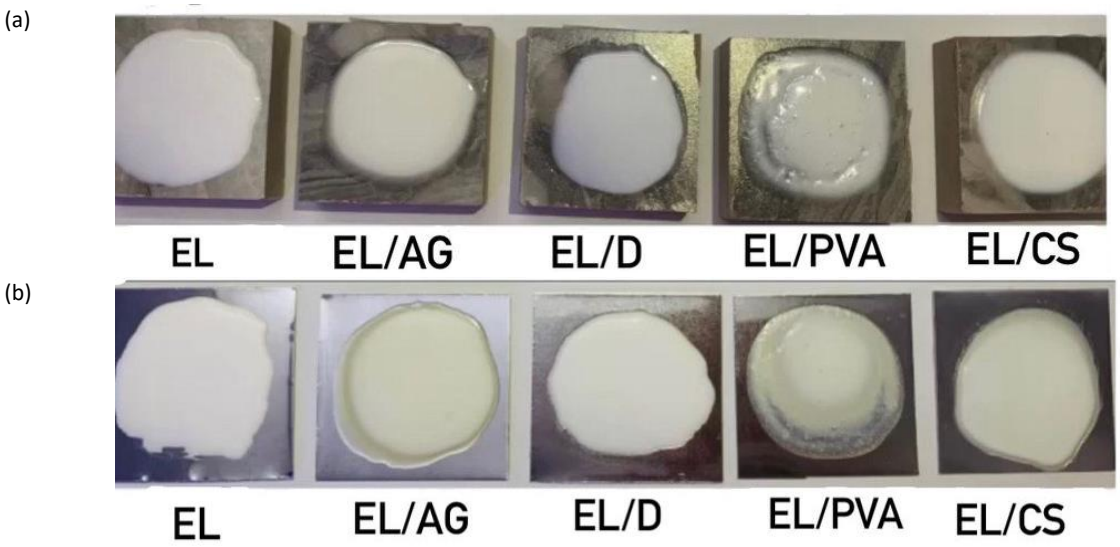

Figure 1. EL, EL/AG, EL/D, EL/PVA, and EL/CS blends prepared for the pull-off adhesion test with **(a)** HDF wood and **(b)** Al substrates.

Single-Lap joints were mechanically evaluated in Quasi-Static conditions using an Intron 4502 electromechanical tensile testing device. In compliance with ASTM D 1002 standard, cross-head speed was set at 1.3 mm min^{-1}. Each sample was subjected to at least six evaluations and the test was performed at RT. A Single-Lap joint may exhibit stiff adhesion and act as a solid with linear elastic properties, according to a shear strength theory. Following these hypotheses, the adhesive will experiences pure shear stress, which is fixed across the entire overlapping range. **Fig. 2** presents the illustration blends for HDF wood and Al substrates.

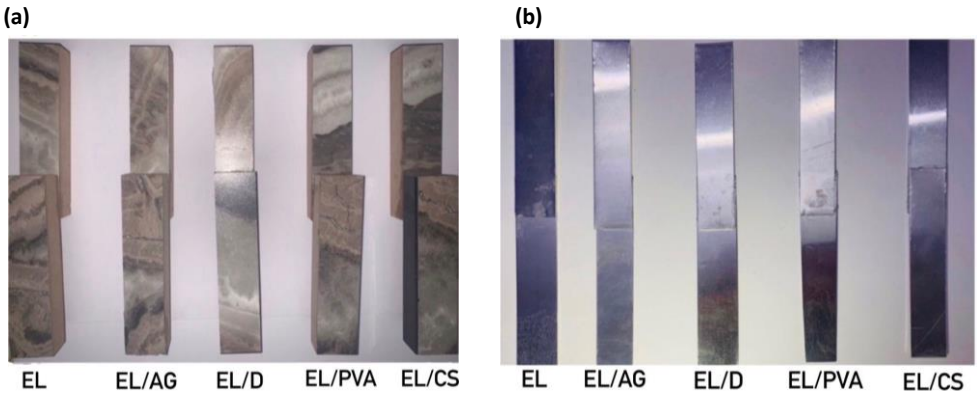

Figure 2. EL, EL/AG, EL/D, EL/PVA, and EL/CS blend samples for **(a)** HDF wood and **(b)** Al substrates.

The sessile drop method is utilized to determine WCA and hence the surface wettability. The liquid droplet (typically water) is produced with a syringe pump, and then the WCA was examined using a camera. The WCA of the droplet on the substrate is identified and calculated by software attached to the camera for 10 s and measured more than 100 times and the average was estimated. Surface roughness, a measure of rough surface, is the vertical deviation of a physical surface from its homogeneous ideal shape. The crucial function that roughness plays in numerous processes, including friction and adhesion, is frequently measured.

A Konica CM-3600d colorimeter was used to determine color coordinates in the CIELAB color space L* (lightness), a* (redness: green to red), and b* (yellowness: blue to yellow). The following equation was used to estimate the average values of total color change (ΔE) for the investigated polymers (Kubo *et al.*, 2013):

$$\Delta E = \sqrt{(a^* - a)^2 + (b^* - b)^2 + (L^* - L)^2} \quad (1)$$

where L*, a*, and b* are standard values meanwhile L, a, and b are the values of investigated samples.

The thermal conductivity coefficient (K), thermal insulation, and passing thermal energy (e) were calculated using Lee's formula. The methods are further explained in our earlier study (Ali *et al.*, 2021). The value of K was determined using the following equations (Hussein *et al.*, 2020; (Al-Sharuee, 2019):

$$K = \frac{e d_s}{T_B - T_A}\left[T_A + \frac{2}{r}\left(d_A + \frac{d_s}{4}\right)T_A + \frac{d_s T_B}{2r}\right. \quad (2)$$

where *e* is the amount of thermal energy passing through a unit area per second through a disk sample and estimated by (Hussein *et al.*, 2020; (Al-Sharuee, 2019):

DOI:https//doi.org/10.22452/mjs.vol43no3.10
Malaysian Journal of Science 43(3): 86-97 (September 2024)

$$e = \frac{IV}{\pi r^2(T_A+T_B)+2\pi r[d_A T_A+\frac{d_S(T_A+T_B)}{2}+d_B T_B+d_C T_C]} \quad (3)$$

here T_A, T_B, and T_C are the temperature (°C) of the disks A, B, and C, meanwhile, d_A, d_B, and d_C are their thicknesses (Hussein *et al.*, 2020), respectively. The IV is the thermal energy transfers through the heating coil unit, *r* is the radius of the disk (mm), and d_s is the thickness of the sample (mm).

The disc diffusion technique with Muller-Hinton agar was used to assess the materials' in vitro antibacterial activity. Sample membranes were sliced into 6 mm diameter discs, which were then put on the bacterial culture, and an inhibitory zone measurement are performed in millimeters (mm) scale. For mixed adhesives, the samples were examined at 37 °C for 6 h against Gram-negative bacteria Escherichia coli (E. coli) and Gram-positive Staphylococcus aureus (S. aureus).

Plasma Surface Treatment

The plasma is generated by a system consisting of a quartz tube (T-shaped) with two entrances: the first to enter the high-voltage electrode, while the second entrance to enter the Ar gas and an outlet for the generated plasma torch. In this setup, the flow rate of pure Ar gas is controlled by a flowmeter. Optical emission spectroscopy (OES) was applied to diagnose the Ar plasma jet by electronically observing the excited species and their intensities in the discharges generated by the dielectric barrier discharge plasma Jet. Surwit device model S3000-UV-NIR was used to record the spectra with a range of 250-950 nm. The optical fiber was placed 1 cm away from the plasma torch and was inclined at an angle of 45°.

3. Results and Discussion

FTIR Analysis

Fig. 3 depicts the FTIR spectra used to describe the structure of the EL and EL/blends. The main observed peaks in the FTIR for EL are located at 3440.8, and 3431.1 cm^{-1} corresponding to sp C–H stretching. The detected bands at 2999.1-2879 cm^{-1}, and 1573.8 cm^{-1} are ascribed to a long chain of $–CH_2$- group and C=C stretching mode of the aromatic ring, respectively. In addition, the bands at 646, 1012.5 cm^{-1} are attributed to C–O which are commonly used as the fingerprint region of liquid rubber (Gharde *et al.*, 2015). The FTIR spectrum of the EL/AG blend showed bands at 3436.9 and 3286.4 cm^{-1}, which are characteristics of the O–H stretching vibration. The detected bands at 3213.1 cm^{-1}, 2960 cm^{-1}, and 2341 cm^{-1} are designated to sp^2 C–H stretching, sp^3 C–H stretching, and C–H stretching, respectively. The C=C bond can be detected at 1413.7, and 1639.3 cm^{-1}, while the C–O–C bending vibrations were observed at 1170, 800.4, 642.2, and 522 cm^{-1}. By inspection of this result, it was observed that the characteristics bands of EL were detected at 3436.9, 2960, 1573.8, and 642.2 cm^{-1}. While the bands at 3286.4, 3213.1, 1639.3, 1413.7, 1170, 800.4, and 522 cm^{-1} are related to the presence of AG in the blend (Petrović et al. 2017). From these results, it was concluded that there is no interaction between AG and EL since there are no new bands are observed and the EL and AG exist in the blend.

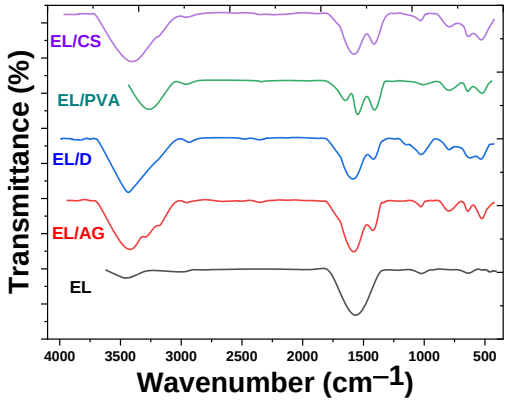

Figure 3. FTIR spectra of EL, EL/AG, EL/D, EL/PVA, and EL/CS blends.

The FTIR spectrum of EL/D polymer showed characteristic bands of EL at 1554, and 1021 cm^{-1}. On the other hand, the characteristics bands of D can be observed at 3432 cm^{-1} (O–H stretching vibration), 2937 cm^{-1} (C–H stretching of the $–CH_2$ group), 1413 cm^{-1} (C–O–H bending mode), 795 cm^{-1} (ring deformation modes of the a-D-(1-4) and a-D-(1-6) linkages), 638 cm^{-1} (the flexural vibration peak of O–H), and 525 cm^{-1} (the bending vibrations of the hydroxide groups outside of their plane (Tohry *et al.*, 2022)). From this result, there is no new bond related to the interaction between EL and D, but the two substances are presented separately in the blend. The FTIR spectrum of EL/PVA displayed bands at 3284 cm^{-1} (O–H stretching), 2955 cm^{-1} (asymmetric stretching of CH_2), 1642 cm^{-1} (O–H bending vibration), 1410 cm^{-1} (CH_2 bending), 800 cm^{-1} (C–C stretching), 648 cm^{-1} (C–H out of plane bending), and 510 cm^{-1} (Kharazmi *et al.*, 2015), which are the characteristics bands of PVA. While the detected bands at 1555 cm^{-1} and 1018 cm^{-1} are the main bands of EL. No new band was detected due to the interaction of EL and PVA, however, they existed in a separate phase in the blend. The FTIR spectrum of EL/CS showed bands at 1554 cm^{-1}, 1021 cm^{-1}, and 647 cm^{-1} are related to EL. In addition, the bands at 3432 cm^{-1} (O–H stretching), 1413 cm^{-1} (C–H symmetrical scissoring of CH_2OH moiety), 804 cm^{-1} (C–O–C ring vibration), and 525 cm^{-1} (Abdullah *et al.*, 2018) belong to CS. Also, there are no new peaks observed for the interaction between CS. Finally, it was concluded from the FTIR results that the bands of EL and other additive polymer exist in the blend, which confirms the successful loading of polymer on the surface of EL.

DOI:https//doi.org/10.22452/mjs.vol43no3.10
Malaysian Journal of Science 43(3): 86-97 (September 2024)

SEM Analysis

Fig. 4 depicts the selected SEM images showing the top view for the EL/AG blend as well as the interface between the EL/AG mix and HDF wood or Al substrates. The homogenous dispersion of the AG within the EL throughout the polymers sample can be shown in **Fig. 4a**. **Fig. 4d** depicts a more enlarged SEM picture (5000×) of the EL/AG blends, demonstrating good dispersion and adhesion between the EL and the AG. The interfaces between the produced mixes and the coated materials, such as HDF wood and Al substrates are shown in **Figs. 4b-f**. The SEM images demonstrate that the EL/AG adheres well to both the HDF wood and the Al substrates.

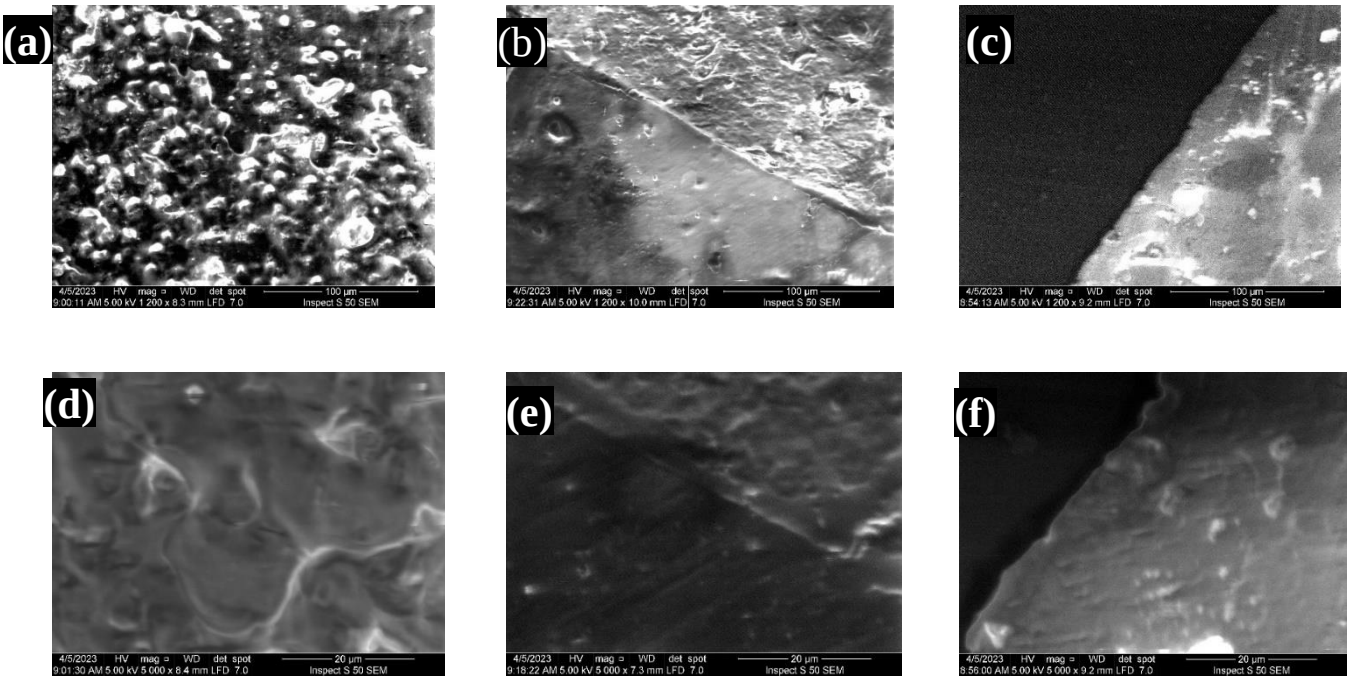

Figure 4. SEM images show the top view with lower (1200×) and higher (5000×) magnifications for **(a, d)** EL/AG blends, and the interface between EL/AG and **(b, e)** HDF wood, or **(c, f)** Al substrates.

Shear Strength

The average values of estimated shear strength, with the error bar, of HDF wood and Al bound with various adhesives are shown in **Fig. 5**. The shear strength of EL is increased by the mixing of various additives to the EL polymer. The maximum values for the shear strength are 771±11, and 52±3 N were observed for the EL/AG polymer at the HDF wood substrate and Al substrates, respectively. In addition, a considerable increase in the characteristics of the adhesive and an improvement in the mechanical performance of the adhesive result from the addition of polymers to the EL and the creation of a homogenous mixture. The best-formed polymer with high mechanical strength and adhesion is EL/AG, accordingly, AG could be the ideal mix. Such observations could be attributed to the characteristics of AG as compared to pure EL polymer. Besides, the strong binding and stabilizing qualities are seen in adhesives of high quality and strength (Baraya *et al.*, 2020). Due to its adhesive qualities and rapid drying time, dextrin follows good adhesion and strength after the AG (Azeez, 2005). Additionally, the combination produced a cross-linking between them that increased the shear strength of HDF wood joined with various adhesives. The shear strength data show a significant difference between Al and HDF wood, as their values are greater for HDF wood compared to Al substrates. The qualities of the wood are to blame for this variation in the outcomes. Its cells have openings that are large enough to provide a clear path for the liquid resin to travel through, and frequently enough, interconnected pits are adequate to encourage resin flow. Hardwood species have high porosity and include vessel and longitudinal fibers. The effectiveness of the bonding between HDF wood pieces depends significantly on how much adhesive reaches the porous network of interconnected cells. Since adhesive bonds move under stress from one component to another through the interphase area. The interphase geometry also affects the bonding performance. Cohesive force promotes chain contact and minimizes free volume, improving the bond strength with the surface of the HDF wood. As for Al, it has a smooth surface, and this makes the adhesion of the mixture to the surface weak (Vineeth *et al.*, 2020).

DOI:https//doi.org/10.22452/mjs.vol43no3.10
Malaysian Journal of Science 43(3): 86-97 (September 2024)

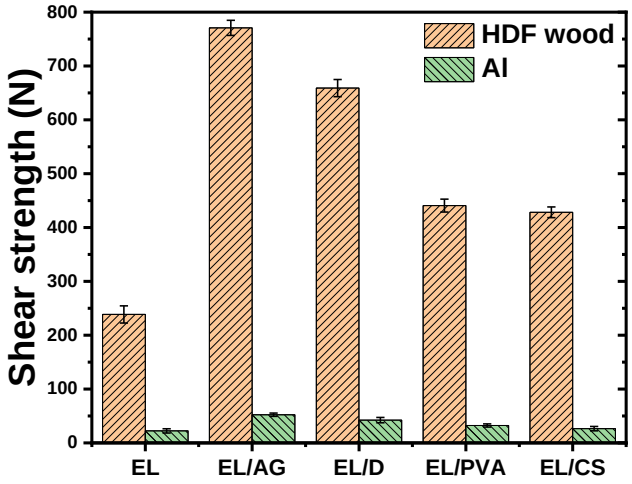

Figure 5. Shear strength of EL, EL/AG, EL/D, EL/PVA, and EL/CS blends.

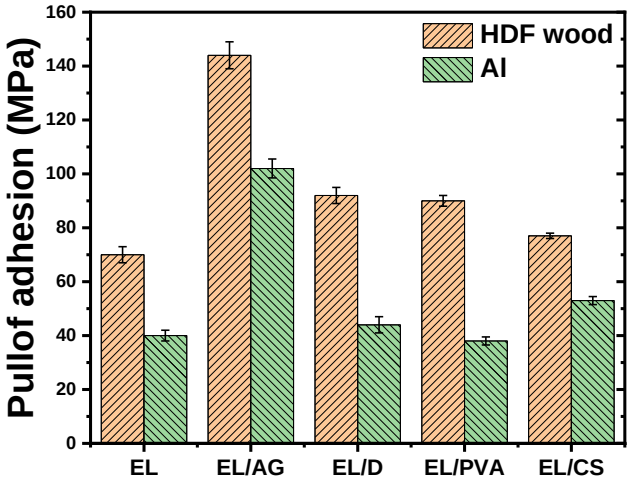

Figure 6. Pull-off adhesion for EL, EL/AG, EL/D, EL/PVA, and EL/CS blends.

Pull off Strength

The adhesive properties have been optimized for the adhesion of EL and EL/blends to the substrate using the pull-off test. **Fig. 6** illustrates the average values of estimated pull-off adhesion, with the error bar, of HDF wood and Al substrates, bonded with different adhesives. According to **Fig. 6**, the highest adhesion value of the material was obtained for EL/AG blend. The distinctive adhesion properties of EL/AG could be attributed to the high adhesive quality, high strength, strong binding, and stabilizing properties of AG (Baraya *et al.*, 2020). It is followed by EL/D and EL/PVA, respectively, with very close values because of the comparable properties of D and PVA. Dextrin has distinctive adhesion properties, in addition to that it dries quickly (Azeez, 2005). PVA is a polymer that is water-soluble and biodegradable and has exceptional adhesion properties. Consequently, PVA is considered one of the promising water-based adhesives and its combination with other polymers could enhance its adhesive capabilities (Azeez, 2005). It was noticed, a large discrepancy between Al and HDF wood in the Pull off results, as a significant and noticeable increase appeared in HDF wood, and these results decreased in Al. The discrepancy in results is due to the properties of the HDF wood. Hardwood species include extremely porous wood, longitudinal fibers, and vessels, cell cavities large enough to provide a favorable conduit for the flow of liquid resin, and connected pits that are frequently large enough to allow the resin to flow (Sultan *et al.*, 2022). The interphase geometry has an impact on the bond performance since the adhesive bonds under pressure migrate from one component to another component across the interphase area. Also, the effectiveness of the bonding between HDF wood components depends on how deeply the adhesive penetrates the porous network of interconnected cells. Cohesive force interacts with the chains and reduces the free volume to tighten the link between them and the wood's surface. As for Al, it is distinguished by its smooth surface, which makes the adhesion of the mixture to the surface weak as mentioned in the shear strength test which agrees with other work elsewhere (Bryaskova *et al.*, 2013).

Color Intensity

A colorimetry study was performed to evaluate and quantify the color deviation of the EL and EL blends. The mean deviation of the CIELab coordinates L*, a*, b*, and ΔE (color difference) are summarized in **Table 1**. The value L* of EL blends decreased compared with LE which indicates that the color adhesives have become darker. However, a*, and b* are the values of EL blends increased compared with EL, so the adhesives blend become more reddish and bluish. The technique of mixing increased the color's intensity as seen in **Table 1**. The formation of conjugated double bonds between the polymer and the modified substance is the fundamental cause of coloring. This yields instauration, which in turn induces electron excitation levels in the visible spectral range and gives discoloration.

Table 1: values of L*, a*, b*, and ΔE for EL, EL/AG, EL/D, EL/PVA, and EL/CS blends

Sample	L*	a*	b*	ΔE
EL	38.78	0.98	5.20	--
EL/AG	34.32	2.21	9.41	6.25
EL/D	29.73	1.86	6.13	9.139
EL/PVA	30.78	0.76	4.22	8.06
EL/CS	32.53	1.92	5.44	6.32

DOI:https//doi.org/10.22452/mjs.vol43no3.10
Malaysian Journal of Science 43(3): 86-97 (September 2024)

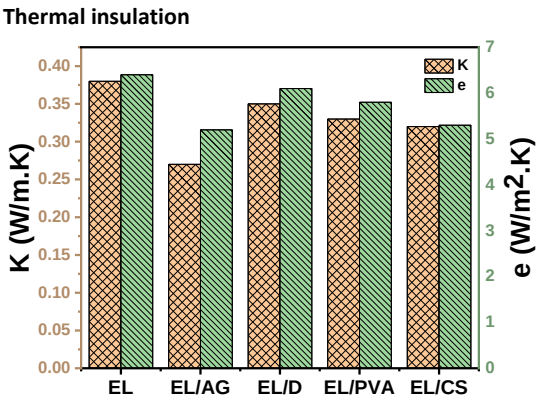

Figure 7. Thermal insulation (K) and passing thermal energy (e) of EL polymer and polymer blend.

Fig. 7 depicts the thermal insulation (K) and passing thermal energy (e) through EL and EL mixtures. In general, both K and e are lowered in EL/blends when compared to pure EL. EL/AG had the lowest observed values for K (0.27 W/m.K) and e (5.2 $W/m^2.K$), indicating good insulation when compared to other examined polymers. The enhanced thermal insulation of EL/AG could be due to the good bonding that occurs between the EL and AG. It is well known that the thermal conductivities of ceramic and metallic materials are orders of magnitude greater than those of polymeric materials (Vlassov *et al.*, 2022). Therefore, there is a need for agglomerations dispersed throughout the polymer blend to improve their thermal conductivity and hence allow for easy heat transmission via the densely packed matrix. Subsequently, when the overall material's solid content grew, decreasing porosity may be connected to higher thermal conductivity. Nonetheless, because of the lower porosity brought on by the denser packing after addition, the weight ratio of polymer to EL liquid improves their mechanical and thermal durability. Polymers combine a two-dimensional structure that vibrates to transfer heat, hence easing the transfer of heat across the material. Polymers are thermally insulators because polymers have a random chain structure and free space exists between chains. The rate of heat transfer in solids depends on whether the material is conductive or insulator (Wang *et al.*, 2022). Irregularity in the structure and the presence of voids between the strings lead to making the insulation process. Accordingly, the transfer of thermal energy from one end to the other through the polymer is difficult, considering the existence of Interfaces between the two phases of the polymeric mixture. The heat is transmitted in the form of elastic phonons within the structure and the presence of interfaces will obstruct the movement and passage of these waves, so the wave will lose part of its energy at the inter-mixture interface as shown in **Fig. 7**.

Anti-bacterial Activity

Investigation of the antibacterial properties of EL is very important because EL can degrade under working conditions due to environmental factors like mechanical stress, heating and cooling, chemicals, and hydrolysis, making the polymer susceptible to bacterial contaminations or infections that pose a serious threat to people (Suethao *et al.*, 2022). Antibacterial for EL mixed adhesives; decrease against initial bacterial loading for S. aureus and E. coli. By using the Agar diffusion technique, EL and mixes are evaluated for their antibacterial activity against the bacterial pathogens S. aureus (gram-positive) and E. coli (gram-negative). **Table 2** and **Fig. 8** both display the zone of inhibition values found for EL and mixed adhesives. Both bacteria were significantly inhibited from growing by the EL/D combination. Antibacterial pictures show more antibacterial efficacy against E. coli bacteria than S. aureus. AG had a bacterial-killing action (Jaafar, 2019). The substantial antibacterial efficacy of Sudanese and Omani AG against S. aureus, and E. coli was investigated (Al Alawi *et al.*, 2018). It was found that the high concentration of non-polar components is thought to be responsible for the antibacterial activity. Both AG and D have also long been used in the food industry and as adhesives, working as an antimicrobial towards gram-positive and gram-negative bacteria in commonly used products such as adhesives of HDF wood.

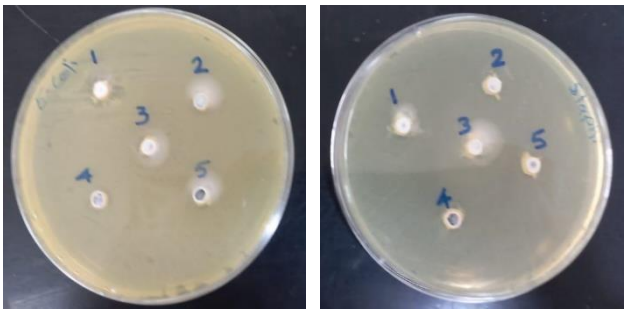

(a) **(b)**

Figure 8. Anti-bacterial activity of EL and EL blends towards **(a)** *E. coli* and **(b)** *S. aureus* bacteria.

Table 2: Zone of inhibition values, in mm, for EL and EL blends towards the tested S. aureus and E. coli organism.

No.	Samples	Bacterial pathogens	
		E. coli	S. aureus
1	EL	13	12
2	EL/AG	14	11
3	EL/D	13	15
4	EL/PVA	11	11
5	EL/CS	13	11

DOI:https//doi.org/10.22452/mjs.vol43no3.10
Malaysian Journal of Science 43(3): 86-97 (September 2024)

Plasma Treatment for Surface Wettability

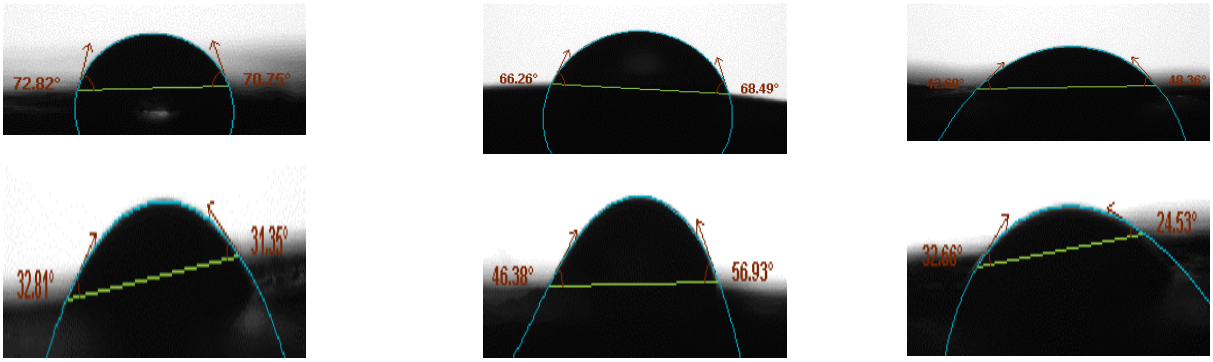

EL **EL/D** **EL/CS**

Figure 9. Seleceted WCA for EL, EL/D, and EL/CS blends before (top images) and after (bottom images) plasma treatment.

The hydrophilic/hydrophobic character of the sample's surface was evaluated by estimating the WCA. **Fig. 9** displays the selected photos showing the WCA for various samples before and after plasma treatment. **Table 3** illustrates the average calculated WCA for various samples before and after the surface treatment using a plasma jet. The backbone of the AG had OH groups, which increased the WCA of the EL/AG combination. The AG polar groups were reduced by the EL, which made it transition from a hydrophilic to a hydrophobic substance. As a result of their combination with the EL groups, these groups decreased. The presence of AG content causes higher WCA values. This expected trend might be caused by the amphiphilic nature of the AG composition. The observed performance may be attributable to the amphiphilic moieties in the structure of AG, specifically an arabinogalactan-protein fraction that comprises both hydrophobic polypeptide chains and hydrophilic polysaccharide blocks, which provide the material's remarkable interfacial properties (do Nascimento *et al.*, 2021).

Table 3: left WCA (θ_1), right WCA and (θ_2), and average WCA ($\bar{\theta}$) of EL and EL blends before and after plasma treatment.

Plasma treatment	**Before**			**After**		
Samples	**θ_1 (°)**	**θ_2 (°)**	**$\bar{\theta}$ (°)**	**θ_1 (°)**	**θ_2 (°)**	**$\bar{\theta}$ (°)**
EL	72.7±0.3	70.6±0.4	71. 7±0.4	31.6±0.7	29.7±0.8	30.7±0.7
EL/AG	83.7±0.5	82.6±0.6	83.2±0.6	45.5±4.5	44.8±8.6	45.2±6.5
EL/D	65.2±1.5	67.6±1.8	66.4±1.6	49.0±2.8	60.6±3.2	54.8±3.0
EL/PVA	85.3±0.3	85.3±0.3	85.3±0.3	69.1±0.4	69.0±0.9	69.1±0.4
EL/CS	41.6±0.9	48.5±0.6	45.0±0.7	33.0±0.2	24.3±0.2	28.6±0.1

DOI:https//doi.org/10.22452/mjs.vol43no3.10
Malaysian Journal of Science 43(3): 86-97 (September 2024)

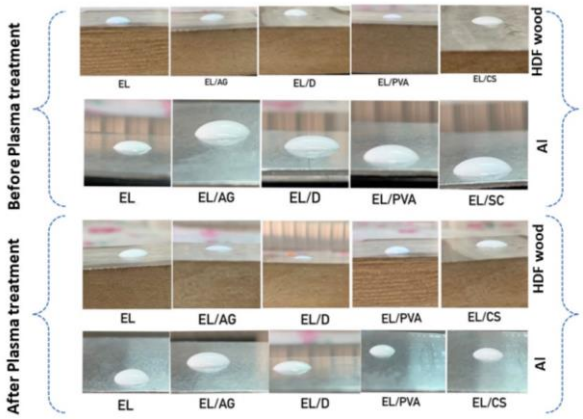

Figure 10. Optical images of droplets of adhesive on HDF wood and Al substrates for EL, EL/AG, EL/D, EL/PVA, and EL/CS blends.

The droplets of EL and EL blend adhesive before and after the plasma treatment over the HDF wood and Al substrates are shown in **Fig. 10**. **Table 4** summarises the estimated average values for contact angle (CA) of EL and EL blends adhesive with HDF wood and Al substrates before and after plasma jet treatment of respective surfaces. The CA for various adhesives is often higher for Al substrates than for HDF wood. Furthermore, plasma treatment reduced CA values for both HDF wood and Al substrates. Following the plasma treatment, the EL/D adhesive with HDF wood had the lowest CA of 38°. The polymer surface displayed perfect hydrophilicity with the adhesive fluids after plasma surface treatment, which decreased the CA starting to raise the surface-based plasma beam's energy. According to Fowkes' theory for calculating surface energy, the rate at which the dispersive and polar surface energies vary is connected to the change in CA. When the treatment impact on the phenomena degraded, the surface polar energy component declined and the dispersive component rose. Conversely, when the CA was low, the polar component of the interfacial energy of the treated sample increased dramatically. This may be explained by the fact that the surface's polar component is increased by a plasma treatment because the plastic's surface forms hydroxyl and carboxyl groups (Miklós & Zoltán, 2021).

Table 4: Average contact angle (CA) of EL and El blends adhesive with HDF wood and Al substrates before and after plasma treatment.

Plasma treatment	substrate	EL	EL/AG	EL/D	EL/PVA	EL/CS
Before	HDF wood	58°	54°	56°	49°	53°
	Al	72°	67°	64°	68°	58°
After	HDF wood	53°	46°	38°	47°	42°
	Al	65°	61°	62°	64°	53°

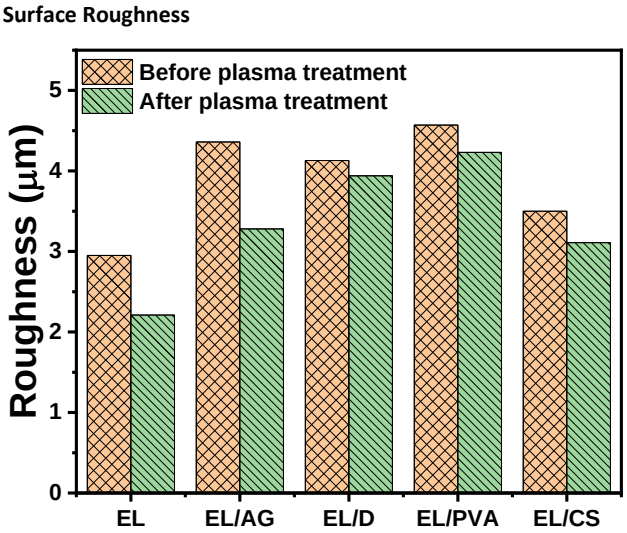

Figure 11. Surface roughness of EL and EL blends before and after plasma treatment.

The relationship between the surface roughness and WCA is that the surface roughness rises as the WCA rises. **Fig. 11** shows the surface roughness of EL and polymer blends before and after plasma treatment. We note that the highest value of roughness was for the non-plasma treated EL/PVA blend, where it was equal to 4.57 µm, and this conforms to the WCA test, where we obtained a high value for the same blend. The roughness ratio of pure PVA was low, and when blend with EL, its surface roughness increased, this means that the elastomer improved the properties of EL polymer which agrees with other work (Vacher & de Wijn, 2021). As well for AG, its properties have been improved and its surface roughness has become equal to 4.36 µm after blending it with EL. Where we obtained similar results in the WCA test for this blend. Accordingly, which agrees with (Sinkhonde, 2023). Also, the blend of EL/D showed a high roughness ratio equal to 4.13 µm, while EL/CS blend has a roughness ratio of 3.5 µm which agrees with other work (Sinkhonde, 2023). When plasma is applied to the surface, the surface becomes less rough, and this can be seen from the WCA values after the surface has been treated with plasma shown in **Fig. 11**.

The surface roughness of El and EL blends is dramatically changed by plasma jet treatment. Roughness values for EL/PVA, EL/D, EL/AG, EL/CS, and EL are 4.23, 3.94, 3.28, 3.11, and 2.21 µm, respectively. The largest drop in surface roughness ratio was obtained for EL (25.1%), while the least decrease (4.6%) was observed for EL/D. In comparison to a non-treated surface, plasma jet treatment of polymer surfaces resulted in a smooth surface. The surface can absorb the EL and EL blends adhesive with excellent efficiency and uniformity throughout its surface due to the reduced surface roughness modified by plasma treatment.

DOI:https//doi.org/10.22452/mjs.vol43no3.10
Malaysian Journal of Science 43(3): 86-97 (September 2024)

4. Conclusion

Various EL blends were prepared to be used for HDF wood and Al coating and adhesion. The filler dispersion and adhesion between the mixtures, coated HDF wood, and Al substrates were validated by SEM analysis. It was concluded from the FTIR results that the bands of EL and other additive polymer exist in the blend, which confirms the successful loading of polymer on the surface of EL. EL integrated with the adhesive's polymer (such as AG, D, PVA, and CS) to high pull-off strength was recorded to be 144 MPa and higher shear strength is 770.8 N for HDF wood as a substrate and 102 MPa, and 52.36 N, respectively, for Al substrates towards the EL/AG. The value L* of blends decreased compared with LE which indicates that the color adhesives have become darker. However, the values of a* and b* for the EL blends increased compared with pure EL, so the adhesives blend become reddish and bluish. The modified EL blend reveals a 0.27 W/m.K for thermal conductivity for EL/AG revealing better thermal insulation than other samples. Antibacterial activity for blended adhesives; decrease against initial bacterial loading for S. aureus and E. coli. Also, AG and D have long been used in the food industry and adhesives, working as an antimicrobial against gram-positive and gram-negative bacteria in commonly used products such as adhesives and coatings. The roughness and wettability of the surface of EL and EL blends were reduced by using a plasma jet, increasing the surface's hydrophilicity. As a result, the surface will be wetter for the adhesive and smoother overall. An alternate biopolymer material was chosen in this investigation because formaldehyde glue is one of the causes of cancer. The addition of EL to common adhesives such as PVA, CS, D, and AG was utilized to alleviate shortcomings such as low water resistance, resistance to conditions, and wet workability. The combination of EL and these natural adhesives improves its water resistance, resistance to conditions, and workability in wet environments. Furthermore, the physical, mechanical, and biological properties of the prepared EL/blends adhesive mixture were improved. It was found that the EL/blends adhesive has greater quality specifications with wood than with aluminum because the wood surface criteria are different from the Al specifications.

5. Acknowledgment

The authors would like to express their gratitude to the Materials Science, Department of Physics, College of Science, University of Baghdad for their assistance, funding, and support. The authors would like to thank Dr. Mohamed Abd El-Aal (Chemistry Department, Faculty of Science, Assiut University, Egypt) for his help.

6. References

Abd-Elnaiem, A. M., Hussein, S. I., Ali, N. A., Hakamy, A., & Mebed, A. M. (2022). Ameliorating the Mechanical Parameters, Thermal Stability, and Wettability of Acrylic Polymer by Cement Filling for High-Efficiency Waterproofing. *Polymers*, 14(21), 4671.

Abdullah, A. Q. , Ali N. A. , Hussein , S. I., Hakamy, A., · Abd-Elnaiem, A. M. (2023) Improving the Dielectric, Thermal, and Electrical Properties of Poly (Methyl Methacrylate)/Hydroxyapatite Blends by Incorporating Graphene Nanoplatelets . Journal of Inorganic and Organometallic Polymers and Materials, published online 28 may 2023.

Al Alawi, S. M., Hossain, M. A., & Abusham, A. A. (2018). Antimicrobial and cytotoxic comparative study of different extracts of Omani and Sudanese Gum acacia. *Beni-Suef University Journal of Basic and Applied Sciences*, 7(1), 22-26.

Ali, A. M., Jaber, M. A., & Toama, N. A. (2021). Thermal Properties of Polyester/Epoxy Blend. *Iraqi Journal of Science*, 1128-1134.

Ali, A. N. M., Ali, N. A., Hussein, S. I., Hakamy, A., Raffah, B., Alofi, A. S., & Abd-Elnaiem, A. M. (2023). Nanoarchitectonics of silver/poly (methyl methacrylate) films: structure, optical characteristics, antibacterial activity, and wettability. *Journal of Inorganic and Organometallic Polymers and Materials*, 33(3), 694-706.

Ali, N. A., Abd-Elnaiem, A. M., Hussein, S. I., Khalil, A. S., Alamri, H. R., & Assaedi, H. S. (2021). Thermal and mechanical properties of epoxy resin functionalized copper and graphene hybrids using in-situ polymerization method. *Current Nanoscience*, 17(3), 494-502.

Al-Lhaibi, S. A., & Al-Shabander, B. M. (2022). Photocatalytic Activity and Wettability Properties of ZnO/Sawdust/Epoxy Composites. *Iraqi Journal of Physics*, 20(4), 54-65.

Almashhadani, N. J. H. (2021). UV-Exposure effect on the mechanical properties of PEO/PVA blends. *Iraqi Journal of Science*, 1879-1892.

Al-sharuee, I. F. (2019). Thermal conductivity performance of silica aerogel after exposition on different heating under ambient pressure. *Baghdad Science Journal*, 16(3 (Suppl.)), 0770-0770.

Awaja, F., Gilbert, M., Kelly, G., Fox, B., & Pigram, P. J. (2009). Adhesion of polymers. *Progress in Polymer Science*, 34(9), 948-968.

AZEEZ, O. (2005). Production of Dextrins from Cassava Starch. *Leonardo Journal of Sciences*, (7), 9-16.

Baraya, K. A., Boryo, D. E. A., Chindo, I. Y., & Hassan, U. F. (2020). Formulation and Characterization of Green Adhesive Using Agricultural and Plastic Waste Materials as Composites. *IOSR Journal of Applied Chemistry* (IOSR-JAC).

DOI:https//doi.org/10.22452/mjs.vol43no3.10
Malaysian Journal of Science 43(3): 86-97 (September 2024)

Berczeli, M., & Weltsch, Z. (2021). Enhanced wetting and adhesive properties by atmospheric pressure plasma surface treatment methods and investigation processes on the influencing parameters on HIPS polymer. *Polymers*, 13(6), 901.

Bryaskova, R., Georgieva, N., Andreeva, T., & Tzoneva, R. (2013). Cell adhesive behavior of PVA-based hybrid materials with silver nanoparticles. *Surface and Coatings Technology*, 235, 186-191.

Chen, X., Sun, C., Wang, Q., Tan, H., & Zhang, Y. (2022). Preparation of glycidyl methacrylate grafted starch adhesive to apply in high-performance and environment-friendly plywood. *International Journal of Biological Macromolecules*, 194, 954-961.

Christenson, E. M., Anderson, J. M., Hiltner, A., & Baer, E. (2005). Relationship between nanoscale deformation processes and elastic behavior of polyurethane elastomers. *Polymer*, 46(25), 11744-11754.

do Nascimento, F. C., de Aguiar, L. C. V., Costa, L. A. T., Fernandes, M. T., Marassi, R. J., Gomes, A. D. S., & de Castro, J. A. (2021). Formulation and characterization of crosslinked polyvinyl alcohol (PVA) membranes: effects of the crosslinking agents. *Polymer Bulletin*, 78(2), 917-929.

Ebewele, R. O. (2000). Polymer science and technology. *CRC press*.

Gharde, R. A., Mani, S. A., Lal, S., Khosla, S., & Tripathi, S. K. (2015). Synthesis and characterization of liquid crystal elastomer. *Materials Sciences and Applications*, 6(06), 527.

Hameed, N. J. (2016). Studying the effect of silica (SiO_2) addition on the adhesive properties of polyvinyl alcohol. *Iraqi Journal of Physics*, 14(29), 107-124.

Henke, M., Lis, B., & Krystofiak, T. (2022). Evaluation of Surface Roughness Parameters of HDF for Finishing under Industrial Conditions. *Materials*, 15(18), 6359.

Hussein, S. I., Ali, N. A., Saleh, G. M., & Jaffar, H. I. (2019). Effect of fiber (Glass, poly propylene) on hardness, water absorption and anti-bacterial activity of coating acrylic polymer. Iraqi Journal of Science, (Special Issue) *The Fourth Conference for Low Dimensional Materials and it's Applications-2018*.

Hussein, S., Abd-Elnaiem, A., Ali, N., & Mebed, A. (2020). Enhanced thermo-mechanical properties of poly (vinyl alcohol)/poly (vinyl pyrrolidone) polymer blended with nanographene. *Current Nanoscience*, 16(6), 994-1001.

Jaafar, N. S. (2019). Clinical effects of Arabic gum (Acacia): A mini review. Iraqi *Journal of Pharmaceutical Sciences* (P-ISSN 1683-3597 E-ISSN 2521-3512), 28(2), 9-16.

Kharazmi, A., Faraji, N., Hussin, R. M., Saion, E., Yunus, W. M. M., & Behzad, K. (2015). Structural, optical, opto-thermal and thermal properties of ZnS–PVA nanofluids synthesized through a radiolytic approach. *Beilstein Journal of Nanotechnology*, 6(1), 529-536.

Kubo, M. T. K., Augusto, P. E., & Cristianini, M. (2013). Effect of high pressure homogenization (HPH) on the physical stability of tomato juice. *Food Research International*, 51(1), 170-179.

Kun, D., & Pukánszky, B. (2017). Polymer/lignin blends: Interactions, properties, applications. *European Polymer Journal*, 93, 618-641.

Mohammed, M. A., Jaber, M. A., & Al-Maamouri, A. F. E. (2022). Study and Evaluation of Rock Wool Board by using PVA/PU as a Polymer Blend Binder. *Iraqi Journal of Science*, 4282-4291.

Parameswaranpillai, J., Thomas, S., & Grohens, Y. (2014). Polymer blends: state of the art, new challenges, and opportunities. *Characterization of Polymer Blends*, 1-6.

etrović, Ž., Ristić, M., Musić, S., & Fabián, M. (2017). The effect of gum arabic on the nano/microstructure and optical properties of precipitated ZnO. *Croatica Chemica Acta*, 90(2), 135-143.

Sinkhonde, D. (2023). Quantitative study on surface porosity and roughness parameters of mineral and organic admixtures based on multi-scale characterisation techniques. *Cleaner Materials*, 7, 100166.

Suethao, S., Prasopdee, T., Buaksuntear, K., Shah, D. U., & Smitthipong, W. (2022). Recent Developments in Shape Memory Elastomers for Biotechnology Applications. *Polymers*, 14(16), 3276.

Sultan, M., Elsayed, H., Abdelhakim, A. E. F., & Taha, G. (2022). Active packaging gelatin films based on chitosan/Arabic gum/coconut oil Pickering nano emulsions. *Journal of Applied Polymer Science*, 139(1), 51442.

Sunday, O. O. (2015). Strength of adhesive bonded joints: Comparative strength of adhesives. *International Journal of Engineering and Technical Research*, 3(8), 58-62.

Tohry, A., Dehghan, R., Hatefi, P., & Chelgani, S. C. (2022). A comparative study between the adsorption mechanisms of sodium co-silicate and conventional depressants for the reverse anionic hematite flotation. *Separation Science and Technology*, 57(1), 141-158.

Vacher, R., & de Wijn, A. S. (2021). Molecular-dynamics simulations of the emergence of surface roughness in a polymer under compression. *Materials*, 14(23), 7327.

DOI:https//doi.org/10.22452/mjs.vol43no3.10
Malaysian Journal of Science 43(3): 86-97 (September 2024)

Vineeth, S. K., Gadhave, R. V., & Gadekar, P. T. (2020). Glyoxal cross-linked polyvinyl alcohol-microcrystalline cellulose blend as a wood adhesive with enhanced mechanical, thermal and performance properties. *Mater Int*, 2, 0277-0285.

Vlassov, S., Oras, S., Timusk, M., Zadin, V., Tiirats, T., Sosnin, I. M., Lõhmus, R., Linarts, A., Kyritsakis, A. & Dorogin, L. M. (2022). Thermal, mechanical, and acoustic properties of polydimethylsiloxane filled with hollow glass microspheres. *Materials*, 15(5), 1652.

Wang, S., Chen, M., & Cao, K. (2022). Polymer composite with enhanced thermal conductivity and insulation properties through aligned Al_2O_3 fiber. *Polymers*, 14(12), 2374.

Zhang, Y., Ding, L., Gu, J., Tan, H., & Zhu, L. (2015). Preparation and properties of a starch-based wood adhesive with high bonding strength and water resistance. *Carbohydrate Polymers*, 115, 32-37.

DOI:https//doi.org/10.22452/mjs.vol43no3.10
Malaysian Journal of Science 43(3): 86-97 (September 2024)